SIAM J. SCI. COMPUT.
Vol. 24, No. 2, pp. 428–442

AN ANALYSIS OF THE ZERO-CROSSING METHOD FOR CHOOSING REGULARIZATION PARAMETERS*

PETER R. JOHNSTON† AND RAMESH M. GULRAJANI‡

Abstract. Solving discrete ill-posed problems via Tikhonov regularization introduces the problem of determining a regularization parameter. There are several methods available for choosing such a parameter, yet, in general, the uniqueness of this choice is an open question. Two empirical methods for determining a regularization parameter (which appear in the biomedical engineering literature) are the composite residual and smoothing operator and the zero-crossing method. An equivalence is established between the zero-crossing method and a minimum product criterion, which has previously been linked with the L-curve method. Finally, the uniqueness of a choice of regularization parameter is established under certain restrictions on the Fourier coefficients of the data in the ill-posed problem.

Key words. discrete ill-posed problems, regularization, parameter choice, L-curve, inverse problem of electrocardiography

AMS subject classifications. 65F22, 65R32

PII. S1064827500373516

1. Introduction.

The inverse problem of electrocardiography [7] is an example of an ill-posed operator equation based on a Fredholm integral equation of the first kind. Here, the electric potential distribution on the surface of the heart is to be determined from measurements of the electric potential on the surface of the body. Due to complex geometries of the thorax and internal organs, the integral equation must be discretized to give a system of linear equations in $\mathbb{R}^m$,

$$\mathbf{A}\phi = \phi_B, \tag{1.1}$$

where $\mathbf{A}$ is an $m \times n$ matrix with a large condition number and, usually, $m \geq n$, ϕ is the required vector of heart surface potentials and ϕ_B is the vector of measured body surface potentials. In this form the inverse problem of electrocardiography is a discrete ill-posed problem. In terms of the Euclidean vector norm in $\mathbb{R}^m$ ($\|\mathbf{x}\|_2 := \sqrt{\mathbf{x}^T\mathbf{x}},\ \mathbf{x} \in \mathbb{R}^m$), least squares minimization [17] of the residuals of (1.1)

$$\min_{\phi \in \mathbb{R}^n} \|\mathbf{A}\phi - \phi_B\|_2^2 \tag{1.2}$$

yields the solution [19]

$$\phi_{LS} = \left(\mathbf{A}^T\mathbf{A}\right)^{-1}\mathbf{A}^T\phi_B, \tag{1.3}$$

where it is assumed that $\mathbf{A}$ is of rank n.

*Received by the editors June 8, 2000; accepted for publication (in revised form) December 10, 2001; published electronically August 15, 2002.
http://www.siam.org/journals/sisc/24-2/37351.html

†School of Science, Griffith University, Nathan, Queensland, 4111, Australia (P.Johnston@mailbox.gu.edu.au). The work of this author was supported by the Australian Research Council.

‡Institute of Biomedical Engineering, Université de Montréal, P.O. Box 6128, Station "Centre–Ville," Montreal, Quebec, H3C 3J7, Canada (gulrajan@igb.umontreal.ca). The work of this author was supported by the Natural Sciences and Engineering Research Council of Canada.

Of course, the above formulation describes many different physical models. However, the reason for introducing the equations in this way is that there are several empirical techniques for studying discrete ill-posed problems in the biomedical literature that do not appear in the mainstream mathematical literature. Here, one of these empirical techniques will be discussed and related to those with a more mathematically sound footing.

There are many different approaches available for solving inverse problems of this type, both in terms of function spaces [5, 6, 13, 20] as well as in the discrete sense [19, 10]. These are but a few examples of many references on this subject. The solutions of these types of equations are based on the so-called regularization methods, probably the most popular of which is that due to Tikhonov and Arsenin [22]. Here, in its simplest form (the zero-order method) a functional (the Tikhonov functional) is constructed by forming a weighted sum of the Euclidean norm of the residuals and the Euclidean norm of the solution

$$\min_{\phi\in\mathbb{R}^n}\left\{\|\mathbf{A}\phi-\phi_B\|_2^2+t\|\phi\|_2^2\right\}, \tag{1.4}$$

where $t\in(0,\infty)$ is called the regularization parameter. The function which minimizes this functional is given by [10]

$$\phi_t=\left(\mathbf{A}^T\mathbf{A}+t\mathbf{I}\right)^{-1}\mathbf{A}^T\phi_B, \tag{1.5}$$

where $\mathbf{I}$ is an $n\times n$ identity matrix.

To obtain a meaningful solution to the minimization problem (1.4), a "good" choice for the regularization parameter t is required. Here again there are several well-established methods which can be employed: the discrepancy principle [5, 6, 20, 22], the generalized cross-validation method [3, 23], and the more recent L-curve approach [8, 10]. In addition, two more heuristic methods have been developed but are generally applied only in the biomedical engineering sphere to the inverse problem of electrocardiography. These are the composite residual and smoothing operator (CRESO) method [2] and the zero-crossing method [14].

In a recent paper, Regińska [21] establishes several results linking the existence of a corner in the L-curve to the existence of a local minimum in the product

$$\Psi_\lambda(t)=\|\mathbf{A}\phi_t-\phi_B\|_2^2\left(\|\phi_t\|_2^2\right)^\lambda \tag{1.6}$$

for some $\lambda>0$. The L-curve is usually a plot of $\log\|\phi_t\|_2^2$ on the ordinate versus $\log\|\mathbf{A}\phi_t-\phi_B\|_2^2$ on the abscissa, and its corner is defined by Hansen and O'Leary [12] as the point of maximum curvature. The t value at the corner serves as the regularization parameter in the L-curve method as both $\log\|\phi_t\|_2^2$ and $\log\|\mathbf{A}\phi_t-\phi_B\|_2^2$ simultaneously attain low values at the corner. Similarly, the t value corresponding to a local minimum of the product $\Psi_\lambda(t)$ serves as an alternative choice for the regularization parameter because $\|\mathbf{A}\phi_t-\phi_B\|_2^2$ and $\|\phi_t\|_2^2$ are increasing and decreasing functions of t, respectively. However, Regińska goes on to state that, in general, the question of the uniqueness of the local minimum of $\Psi_\lambda(t)$ inside $(0,\infty)$ is still open. This paper presents a discussion of the link between the minimum of $\Psi_1(t)$ (i.e., (1.6) with $\lambda=1$; see also [18]) and the zero-crossing method. It formalizes our earlier demonstration [15] that the minimum of $\Psi_1(t)$ and the zero-crossing method both result in identical t values. It also includes a demonstration that, under certain restrictions on the Fourier coefficients of the data, a unique regularization parameter may be chosen for this type of discrete ill-posed problem.

Following this introduction, in section 2 the tools required for the subsequent analysis (namely singular value decomposition) are introduced. Section 3 introduces the two heuristic methods mentioned above, namely CRESO and the zero-crossing method. Section 4 proves two lemmas which link the zero-crossing method to the minimization of the product $\Psi_1(t)$ and, last, section 5 contains two demonstrations of the uniqueness of the regularization parameter for simple spectra of the Fourier coefficients of the data. The paper closes with two illustrative numerical examples.

2. Mathematical preliminaries. To begin the analysis of the ill-posed problem compute the singular value decomposition of the $m \times n$ $(m \geq n)$ forward transfer matrix $\mathbf{A} \in \mathbb{R}^{m,n}$, of which one form is given by [4, 17],

$$\mathbf{A} = \mathbf{U}\Sigma\mathbf{V}^T, \tag{2.1}$$

where $\mathbf{U} \in \mathbb{R}^{m,m}$ and $\mathbf{V} \in \mathbb{R}^{n,n}$ are orthonormal matrices, $\Sigma = \text{diag}(\sigma_1, \sigma_2, \ldots, \sigma_n)$, and $\sigma_1 \geq \sigma_2 \geq \cdots \geq \sigma_n \geq 0$. The σ_i are the singular values of $\mathbf{A}$ and the ith column vectors u_i and v_i of $\mathbf{U}$ and $\mathbf{V}$, respectively, are the left and right singular vectors corresponding to σ_i, $i = 1, 2, \ldots, n$.

Using this singular value decomposition for $\mathbf{A}$, it can be shown (see [14]) that the least squares solution, ϕ_{LS} (1.3), may be written as

$$\phi_{LS} = \sum_{i=1}^{n} \left(\frac{\alpha_i}{\sigma_i} \right) v_i, \tag{2.2}$$

where the α_i denote the Fourier coefficients, given by the scalar products

$$\alpha_i = u_i^T \phi_B, \qquad i = 1, \ldots, n. \tag{2.3}$$

Similarly, the regularized solution, ϕ_t (1.5), can be written as

$$\phi_t = \sum_{i=1}^{n} \left(\frac{\sigma_i \alpha_i}{\sigma_i^2 + t} \right) v_i. \tag{2.4}$$

Hence, it follows that

$$\|\phi_t\|_2^2 = \sum_{i=1}^{n} \frac{\sigma_i^2 \alpha_i^2}{(\sigma_i^2 + t)^2}. \tag{2.5}$$

Further, if the least squares residual vector $b_\perp := \mathbf{A}\phi_{LS} - \phi_B = -\sum_{i=n+1}^{m} \alpha_i u_i$, then it also follows that

$$\mathbf{A}\phi_t - \phi_B = -\sum_{i=1}^{n} \frac{t\alpha_i}{\sigma_i^2 + t} u_i + b_\perp \tag{2.6}$$

and so

$$\|\mathbf{A}\phi_t - \phi_B\|_2^2 = \sum_{i=1}^{n} \frac{t^2 \alpha_i^2}{(\sigma_i^2 + t)^2} + \|b_\perp\|_2^2. \tag{2.7}$$

The above expressions for $\|\phi_t\|_2$ and $\|\mathbf{A}\phi_t - \phi_B\|_2$ are based on the assumption that the coefficient matrix $\mathbf{A}$ is of rank n. However, these expressions are also valid if $\mathbf{A}$ is of rank r $(r \leq n)$ with the upper limit of the summation being r instead of n. For generality, a coefficient matrix $\mathbf{A}$ of rank r will be used in the subsequent analysis of the methods for choosing the regularization parameter t.

3. Two heuristic methods. One heuristic method that is very popular in the electrocardiographic literature is called the CRESO method [2]. The method consists of finding the smallest value of $t > 0$ that results in a relative maximum of the function

$$C(t) = \|\phi_t\|_2^2 + 2t\frac{d}{dt}\|\phi_t\|_2^2 \tag{3.1}$$

which can be evaluated by differentiating (2.5) to yield

$$C(t) = \sum_{i=1}^{r}\left(\frac{\sigma_i\alpha_i}{\sigma_i^2+t}\right)^2\left[1-\frac{4t}{\sigma_i^2+t}\right]. \tag{3.2}$$

While the motivation for the CRESO method is unclear, its name comes from the fact that $C(t)$ is the derivative, with respect to the regularization parameter, t, of the composite function

$$B(t) = -\|\mathbf{A}\phi_t - \phi_B\|_2^2 + t\|\phi_t\|_2^2\,; \tag{3.3}$$

that is to say

$$C(t) = B'(t). \tag{3.4}$$

The first term on the right-hand side of (3.3) represents the residual of (1.1) when the solution ϕ_t is used, and the second term represents the magnitude of the solution ϕ_t. Of course, the function $B(t)$ is simply the difference between the two terms in the Tikhonov functional (1.4). The value of t chosen via the CRESO method corresponds to the first point where $B(t)$ changes concavity (i.e., where the second derivative of $B(t)$ changes sign).

The second heuristic method is also based on the function $B(t)$, but instead of looking for changes of concavity in $B(t)$ we look for the value of t at which $B(t) = 0$; see [14]. This method has been dubbed the "zero-crossing method." Here, the terms of the Tikhonov functional are given an equal weighting; that is, equal emphasis is placed on having a small residual as is placed on having a small norm for the solution, scaled by the regularization parameter. So, in a sense, this argument provides a motivation for the zero-crossing method of choosing a regularization parameter. Extensive testing and numerical experiments of the zero-crossing method in connection with the inverse problem of electrocardiography have been published elsewhere [14, 15, 16], where it was observed that the function $B(t)$ had two zeros, t_1 and t_2, say. The heuristic method developed suggested that the value of t corresponding to the smaller zero, $t = t_1$, should be chosen as the regularization parameter [14]. It was also observed that $B'(t_1) > 0$. This zero-crossing method breaks down when the smaller zero of $B(t)$ disappears, when it occurs so close to $t = 0$ as to be below machine precision. This breakdown was observed under conditions when there was no corner in the L-curve, i.e., under conditions when the latter method also broke down.

By using (2.5) and (2.7), it can be shown that, in terms of the singular value decomposition of the coefficient matrix, $\mathbf{A}$,

$$B(t) = \sum_{i=1}^{r}\frac{t\alpha_i^2(\sigma_i^2-t)}{(\sigma_i^2+t)^2} - \|b_\perp\|_2^2. \tag{3.5}$$

This form of $B(t)$ will be used for all further analysis.

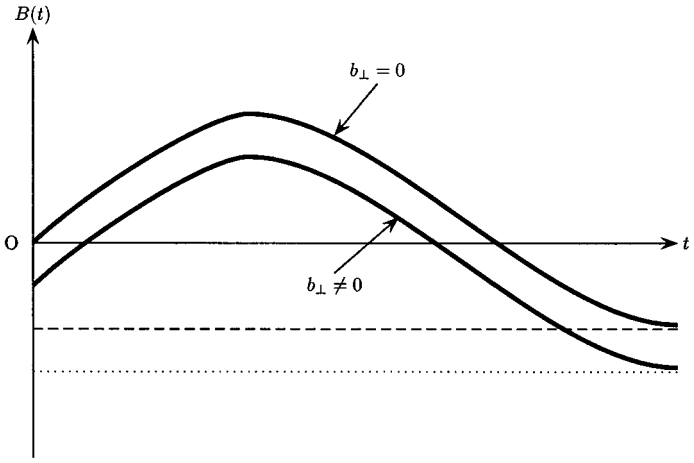

FIG. 1. *Schematic representation of the curve* $B(t)$ (3.5)*, both when* $b_\perp = 0$ *and when* $b_\perp \neq 0$*. The horizontal asymptotes are at values of* $-\sum_{i=1}^{r} \alpha_i^2$ *(dashed line) and* $-\sum_{i=1}^{r} \alpha_i^2 - \|b_\perp\|_2^2$ *(dotted line).*

At this stage it is worth considering some of the properties of $B(t)$. Initially, assume that $\|b_\perp\|_2 = 0$; then clearly, when $t = 0$, $B(0) = 0$. On the other hand, as $t \to \infty$ it can be seen that

$$\lim_{t\to\infty} B(t) = -\sum_{i=1}^{r} \alpha_i^2 < 0, \tag{3.6}$$

and the limit is approached from above. Also, for $0 < t \leq \sigma_r^2$, $B(t) > 0$ and for $t \geq \sigma_1^2$, $B(t) < 0$. Therefore, all zeros of $B(t)$, other than the one at $t = 0$, must occur for values of t such that $\sigma_r^2 \leq t \leq \sigma_1^2$.

Further, (3.5) can be differentiated with respect to t to give

$$B'(t) = \sum_{i=1}^{r} \frac{\alpha_i^2 \sigma_i^2 (\sigma_i^2 - 3t)}{(t + \sigma_i^2)^3} \tag{3.7}$$

which, of course, is $C(t)$ (see (3.2)). Therefore, the slope of $B(t)$ at $t = 0$ is positive and for large values of t it is negative; in fact, $B'(t) < 0$ for $t \geq \frac{\sigma_1^2}{3}$. Based on these observations, the function $B(t)$ must have an even number of zeros (including $t = 0$) and an odd number of turning points on $[0, \infty)$. A postulated form of $B(t)$ (based on considerable numerical experience) is shown in Figure 1. When the restriction that $\|b_\perp\|_2 = 0$ is removed, the whole $B(t)$ curve simply moves downward (Figure 1). Hence, if $\|b_\perp\|_2$ is sufficiently small, it will still be true that $B(t)$ has an even number of zeros.

It is also possible to rewrite (3.5) as

$$B(t) = \sum_{i=1}^{r} B_i(t) - \|b_\perp\|_2^2, \tag{3.8}$$

where

$$B_i(t) = \frac{t\alpha_i^2(\sigma_i^2 - t)}{(\sigma_i^2 + t)^2}. \tag{3.9}$$

Then, for later use, the following can be observed about the functions $B_i(t)$, $i = 1, \ldots, r$:

1. Each $B_i(t)$ has two zeros, at $t = 0$ and $t = \sigma_i^2$.
2. Each $B_i(t)$ has one maximum, at $t = \frac{\sigma_i^2}{3}$ with a value of $\frac{\alpha_i^2}{8}$.
3. $\lim_{t\to\infty} B_i(t) = -\alpha_i^2$ (with the limit approached from above).

4. Links with other techniques. In this section the relationship between the zero-crossing method, the L-curve method [8, 12], and Regińska's local minimum criterion [21, 18] is investigated. As mentioned in the introduction, Regińska [21] has established a link between the existence of a corner in the L-curve and a local minimum of the function $\Psi_1(t)$. The following lemma establishes the equivalence of the zero-crossing method and the local minimum of $\Psi_1(t)$.

LEMMA 4.1. *There exists a local minimum of* $\Psi_1(t)$ *at* $\hat{t} \in (0, \infty)$ *iff* $B(\hat{t}) = 0$ *and* $B'(\hat{t}) > 0$.

Proof. From the definition of $\Psi_\lambda(t)$ (1.6) with $\lambda = 1$

$$\Psi_1(t) = \|\mathbf{A}\phi_t - \phi_B\|_2^2 \|\phi_t\|_2^2 \tag{4.1}$$

$$= \left(t\|\phi_t\|_2^2 - B(t)\right) \|\phi_t\|_2^2 \tag{4.2}$$

from (3.3). Next, differentiating with respect to t gives

$$\frac{d\Psi_1(t)}{dt} = \left(\|\phi_t\|_2^2 + t\frac{d}{dt}\|\phi_t\|_2^2 - B'(t)\right) \|\phi_t\|_2^2 + \left(t\|\phi_t\|_2^2 - B(t)\right) \frac{d}{dt}\|\phi_t\|_2^2 \tag{4.3}$$

$$= \|\phi_t\|_2^2 \left(\|\phi_t\|_2^2 + 2t\frac{d}{dt}\|\phi_t\|_2^2 - B'(t)\right) - B(t)\frac{d}{dt}\|\phi_t\|_2^2 \tag{4.4}$$

$$= \|\phi_t\|_2^2 \left(C(t) - B'(t)\right) - B(t)\frac{d}{dt}\|\phi_t\|_2^2, \tag{4.5}$$

where the last equality follows from (3.1). Further, from (3.4), it follows that

$$\frac{d\Psi_1(t)}{dt} = -B(t)\frac{d}{dt}\|\phi_t\|_2^2 \tag{4.6}$$

$$= 2B(t)\sum_{i=1}^{r} \frac{\sigma_i^2\alpha_i^2}{(\sigma_i^2 + t)^3}, \tag{4.7}$$

obtained by differentiating (2.5) with respect to t. Since the summation term is strictly positive, it follows that

$$\frac{d\Psi_1(t)}{dt} = 0 \text{ iff } B(t) = 0. \tag{4.8}$$

Further differentiation gives

$$\frac{d^2\Psi_1(t)}{dt^2} = -6B(t)\sum_{i=1}^{r} \frac{\sigma_i^2\alpha_i^2}{(\sigma_i^2 + t)^4} + 2B'(t)\sum_{i=1}^{r} \frac{\sigma_i^2\alpha_i^2}{(\sigma_i^2 + t)^3}, \tag{4.9}$$

and therefore, at the point where $B(t) = 0$, we have that

$$\frac{d^2\Psi_1(t)}{dt^2} > 0 \text{ iff } B'(t) > 0. \tag{4.10}$$

Hence the result is established. ∎

Using the result of the above lemma, Lemma 6 from [21] can be recast in terms of $B(t)$.

LEMMA 4.2.

1. *For $b_\perp = 0$: There exists a point $\hat{t} \in (0, \infty)$ such that $B(\hat{t}) = 0$ and $B'(\hat{t}) > 0$ iff $\exists\ t_1, t_2$, with $0 \le t_1 < t_2$ such that $B(t_1) \le 0$ and $B(t_2) \ge 0$.*

2 *For $b_\perp \neq 0$: There exists a point $\hat{t} \in (0, \infty)$ such that $B(\hat{t}) = 0$ and $B'(\hat{t}) > 0$ iff $\exists\ t_2 > 0$ such that $B(t_2) \ge 0$.*

Proof. Note first that $B(t)$ is a continuous function as it is the difference of continuous functions (see (3.3)).

1. For $b_\perp = 0$: If $\exists\ t_1, t_2$, with $0 \le t_1 < t_2$ such that $B(t_1) \le 0$ and $B(t_2) \ge 0$, then by continuity of $B(t)$, $\exists\ \hat{t} \in [t_1, t_2]$ such that $B(\hat{t}) = 0$ and $B'(\hat{t}) > 0$.
On the other hand, if $\exists\ \hat{t} \in (0, \infty)$ such that $B(\hat{t}) = 0$ and $B'(\hat{t}) > 0$, then there exists a small neighborhood of $\hat{t}$, $[t_1, t_2]$ say, such that $B(t) \le 0$ for all $t \in [t_1, \hat{t}]$ and $B(t) \ge 0$ for all $t \in [\hat{t}, t_2]$. Therefore, there exist two points t_1, t_2, with $0 \le t_1 < t_2$ such that $B(t_1) \le 0$ and $B(t_2) \ge 0$.

2. For $b_\perp \neq 0$: Here we can choose $t_1 = 0$ as $B(0) = -\|b_\perp\|_2^2 < 0$, and the proof is as above. ∎

Lemma 4.2 establishes conditions for the existence of a zero of the function $B(t)$ and thus the existence of a regularization parameter which seeks to balance the residual norm against the scaled solution norm. It also suggests some interesting behavior which is required of $B(t)$ for a zero corresponding to such a regularization parameter to exist. Clearly, if $b_\perp \neq 0$, then, since $B(0) < 0$, it follows that $B(t)$ simply crossing the t-axis is sufficient to provide the required regularization parameter. Assuming that there are only two zeros of $B(t)$ in this case (as suggested by the numerical evidence for the inverse electrocardiography problem), then at the left hand zero, t_1 say, $B'(t_1) > 0$. Hence by Lemma 4.1, there is a minimum in $\Psi_1(t)$ at $t = t_1$ and so according to Regińska [21] there exists a corner of the L-curve, albeit not necessarily at t_1. This same choice of regularization parameter, t_1, is also predicted by the heuristic zero-crossing method [14], thus providing a validation for that method as an alternative to the L-curve corner. On the other hand, if $b_\perp = 0$, it is required that there are at least four zeros of $B(t)$ (the first being $t = 0$) with the third being the appropriate choice for the regularization parameter. A situation where $b_\perp = 0$ is when the coefficient matrix, $\mathbf{A}$, is square and of full rank. The two numerical examples in section 6 illustrate results corresponding to $b_\perp \neq 0$ and $b_\perp = 0$, respectively.

By finding the minimum of the more general $\Psi_\lambda(t)$ (1.6), that is, by studying where $\frac{d\Psi_\lambda(t)}{dt} = 0$, it is possible to reformulate Lemma 4.1 in terms of the function $B_\lambda(t)$ defined by

$$B_\lambda(t) := \sum_{i=1}^{r} \frac{t\alpha_i^2(\sigma_i^2 - \lambda t)}{(\sigma_i^2 + t)^2} - \lambda\|b_\perp\|_2^2. \tag{4.11}$$

Further, for a fixed λ, Lemma 4.2 can now be applied to the function $B_\lambda(t)$.

5. Uniqueness in choosing the regularization parameter. In this section, two demonstrations are presented which establish the existence of a unique regularization parameter in terms of zeros of the function $B(t)$ under simplifying assumptions

on the Fourier coefficients of the data. The first is given more rigorously in the form of a theorem, and the second is a more informal demonstration.

Consider a discrete ill-posed problem and a regularized solution ϕ_t obtained via Tikhonov regularization. To establish the uniqueness of t as predicted by the zeros of $B(t)$ under the simplifying assumptions mentioned above, the following three assumptions are required. These are the same three assumptions needed to ensure the existence of a corner in the L-curve [12].

1. The discrete Picard condition is satisfied for the unperturbed problem (with no error in $\mathbf{A}$ or ϕ_B); that is, the coefficients $|\alpha_i|$ on average decay to zero faster than the singular values σ_i, or, more mathematically,

$$\lim_{i\to\infty} \frac{|\alpha_i|}{\sigma_i} = 0. \tag{5.1}$$

2. The errors in the right-hand side of (1.1) are essentially "white noise."
3. The signal-to-noise ratio is reasonably large.

With these three conditions holding, the following theorem can be established for the particular situation where the right-hand side vector, ϕ_B, has only two nonzero Fourier coefficients.

THEOREM 5.1. *Let $i_1 < i_2$ be such that $\alpha_i \neq 0$ for $i \in \{i_1, i_2\}$ and $\alpha_i = 0$ for $i \notin \{i_1, i_2\}$; then the curve $B(t)$ has only two zeros for $t > 0$ and $\|b_\perp\|_2$ sufficiently small and nonzero.*

Proof. The relationship between the singular values says that $\sigma_{i_1} \geq \sigma_{i_2} > 0$ and the discrete Picard condition allows us to assume that $\frac{|\alpha_{i_1}|}{\sigma_{i_1}} \geq \frac{|\alpha_{i_2}|}{\sigma_{i_2}}$, which in turn implies that $|\alpha_{i_1}| \geq |\alpha_{i_2}| \geq 0$. Hence, in this simple case

$$B(t) = \frac{\alpha_{i_1}^2 t(\sigma_{i_1}^2 - t)}{(\sigma_{i_1}^2 + t)^2} + \frac{\alpha_{i_2}^2 t(\sigma_{i_2}^2 - t)}{(\sigma_{i_2}^2 + t)^2} - \|b_\perp\|_2^2. \tag{5.2}$$

To simplify matters even further, assume for the moment that $\|b_\perp\|_2 = 0$, take out a common factor of $\alpha_{i_1}^2$ from the remaining terms of (5.2), and by defining $s = t/\sigma_{i_1}^2$, $\beta = |\alpha_{i_2}|/|\alpha_{i_1}|$, and $\gamma = \sigma_{i_2}/\sigma_{i_1}$ we obtain

$$B(t) = \alpha_{i_1}^2 G(s), \tag{5.3}$$

where

$$G(s) = \frac{s(1-s)}{(1+s)^2} + \frac{\beta^2 s(\gamma^2 - s)}{(\gamma^2 + s)^2} = G_1(s) + G_2(s), \tag{5.4}$$

say. Note that $G_2(s) = \beta^2 G_1(\frac{s}{\gamma^2})$. Due to the above relationships between σ_{i_1}, σ_{i_2}, α_{i_1}, and α_{i_2}, it follows that $0 \leq \beta \leq \gamma \leq 1$. When $\|b_\perp\|_2 = 0$ it must be established that there is only one point $s_0 > 0$ such that $G(s_0) = 0$. The two functions $G_1(s)$ and $G_2(s)$ are shown in Figure 2 for $\beta^2 = 0.7$ and $\gamma^2 = 0.8$ (in panel (a)) and for $\beta^2 = 0.2$ and $\gamma^2 = 0.3$ (in panel (b)). Their properties are the same as for the functions $B_i(t)$, defined in (3.9) and discussed at the end of section 3.

The theorem must be established in two situations: first, when the zero of $G_2(s)$ occurs at a point beyond the maximum of $G_1(s)$, as depicted in Figure 2(a) (i.e., $\gamma^2 \geq \frac{1}{3}$) and, second, when it is before the maximum of $G_1(s)$, as shown in Figure 2(b) (i.e., $\gamma^2 \leq \frac{1}{3}$).

Case 1. ($\gamma^2 \geq \frac{1}{3}$). Here $G_1(s) + G_2(s) > 0$ for $s \leq \gamma^2$ and $G_1(s) + G_2(s) < 0$ for $s \geq 1$.

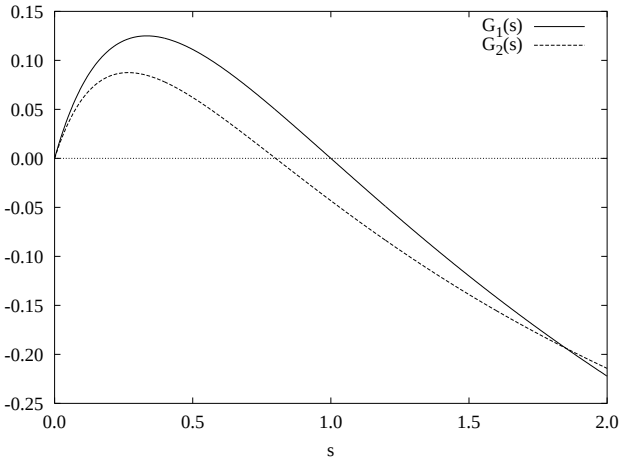

(a) Case 1 (with $\beta^2 = 0.7$ and $\gamma^2 = 0.8$)

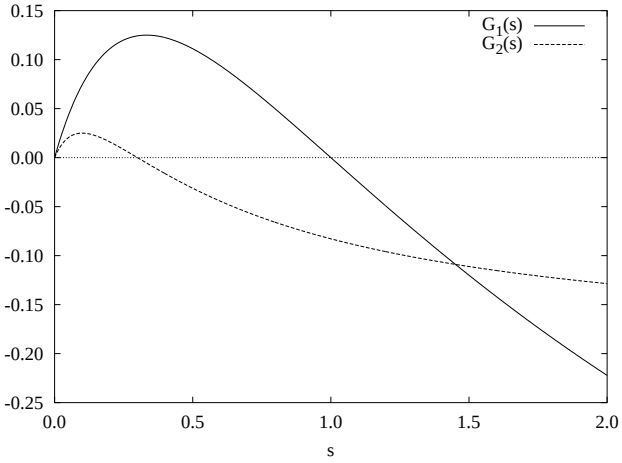

(b) Case 2 (with $\beta^2 = 0.2$ and $\gamma^2 = 0.3$)

FIG. 2. *Plots of the functions $G_1(s)$ and $G_2(s)$ which are components of the function $G(s)$ (5.4).*

Now, consider the interval $I = [\gamma^2, 1]$. At the endpoints of the interval

$$G(\gamma^2) = G_1(\gamma^2) + G_2(\gamma^2) = G_1(\gamma^2) = \frac{\gamma^2(1-\gamma^2)}{(1+\gamma^2)^2} \geq 0 \tag{5.5}$$

and

$$G(1) = G_1(1) + G_2(1) = G_2(1) = \frac{\beta^2(\gamma^2-1)}{(1+\gamma^2)^2} \leq 0. \tag{5.6}$$

(The inequalities follow as $\gamma \leq 1$.) Therefore, there exists at least one zero of $G(s)$ in I. However, $G_1'(s) \leq 0$ for all $s \in I$ and $G_2'(s) \leq 0$ for all $s \in I$; i.e., both functions $G_1(s)$ and $G_2(s)$ are monotonically decreasing on I, and, therefore, so is $G_1(s)+G_2(s)$. Hence there exists a unique zero of $G(s)$ between γ^2 and 1 when $\gamma^2 \geq \frac{1}{3}$.

Case 2 ($\gamma^2 < \frac{1}{3}$). Clearly, $G_2(\frac{1}{3}) < 0$. However, if $G_2(\frac{1}{3}) > -\frac{1}{8}$ ($\frac{1}{8}$ being the maximum value of $G_1(s)$); then $G_1(s) + G_2(s) > 0$ for $0 < s < \frac{1}{3}$; then as in Case 1,

there exists a unique zero between γ^2 and 1 as $G_1(s)$ and $G_2(s)$ are both monotonically decreasing for $s > \frac{1}{3}$.

To complete the proof, it must be shown that $-G_2(\frac{1}{3}) < \frac{1}{8}$. Consider

$$-G_2\left(\frac{1}{3}\right) = \frac{\beta^2 \frac{1}{3}(\frac{1}{3} - \gamma^2)}{(\frac{1}{3} + \gamma^2)^2} = \frac{\beta^2(1 - 3\gamma^2)}{(1 + 3\gamma^2)^2} \tag{5.7}$$

$$\leq \gamma^2(1 - 3\gamma^2) = \frac{1}{12} - 3\left(\gamma^2 - \frac{1}{6}\right)^2 \leq \frac{1}{12} < \frac{1}{8}.$$

So far it has been established that the function $B(t)$, given by (5.2), has only one strictly positive zero for $\|b_\perp\|_2 = 0$. Including a sufficiently small nonzero value of $\|b_\perp\|_2$ has the effect of a downward translation of the function $B(t)$; hence there are only two strictly positive zeros and the result is established. □

Of the two zeros determined from the above result, only one satisfies the conditions of Lemma 4.1. This is the smaller zero, and so the regularization parameter chosen via this method is unique. It therefore follows that the regularization parameter chosen by the heuristic zero-crossing method is also unique, under the assumptions of Theorem 5.1.

The second demonstration of the uniqueness of the regularization parameter is more informal and is based on ideas presented by Hansen [11]. Again, begin with (3.5) and initially assume $\|b_\perp\|_2 = 0$; then $B(t)$ has the form

$$B(t) = \sum_{i=1}^{r} \frac{t\alpha_i^2(\sigma_i^2 - t)}{(\sigma_i^2 + t)^2}. \tag{5.8}$$

Now, introduce the variable $\chi_i = \frac{\alpha_i}{\sigma_i}$; then

$$B(t) = \sum_{i=1}^{r} \frac{t\sigma_i^2\chi_i^2(\sigma_i^2 - t)}{(\sigma_i^2 + t)^2}. \tag{5.9}$$

Further, without loss of generality, it can be assumed that $\sigma_1 = 1$, and only values of t in the range $0 \leq t \leq 1$ are of interest.

At this stage, no way has been discovered to analyze the expression for $B(t)$ given in (3.5). Therefore we follow the idea suggested by Hansen [11]: replace the discrete variables σ_i and χ_i with continuous variables σ and $\chi = \chi(\sigma)$, respectively, replace the summation with an integral, and consider the quantity

$$\Theta(t) = \int_0^1 \frac{t\sigma^2\chi^2(\sigma)(\sigma^2 - t)}{(\sigma^2 + t)^2}\, d\sigma. \tag{5.10}$$

It is expected that the behavior of $\Theta(t)$ will reasonably well approximate the behavior of $B(t)$ and, in particular, both functions are expected to have the same number of zeros.

To further simplify the analysis, it is assumed that χ is a simple function of σ given by

$$\chi(\sigma) = \sigma^p, \tag{5.11}$$

where $p \in \mathbb{R}$. This is not an unreasonable assumption, and it is the basis for many modelling problems [10]. The exponent p characterizes the behavior of the right-hand

side in (1.1) as $u_i^T \phi_B = \alpha_i = \sigma_i \chi_i \sim \sigma^{p+1}$. It can be looked upon as a smoothness parameter since, by controlling the decay of the exact-solution Fourier coefficients, it controls, in a mathematical sense, the smoothness of the exact solution. When $p > 0$, the right-hand side satisfies the discrete Picard condition and for $p < 0$ it does not. In the latter situation, a regularized solution of (1.1) may or may not exist. In particular, $p = -1$ corresponds to a right-hand side consisting of white noise [11]. With the above expression for $\chi(\sigma)$

$$\Theta(t) = \int_0^1 \frac{t\sigma^{2p+2}(\sigma^2 - t)}{(\sigma^2 + t)^2}\, d\sigma. \tag{5.12}$$

Evaluation of this integral is performed by first introducing the change of variable $\mu = \sigma^2$ to give, after some manipulation,

$$\Theta(t) = \frac{t}{2} \int_0^1 \frac{\mu^{p+\frac{3}{2}}}{(\mu + t)^2}\, d\mu - \frac{t^2}{2} \int_0^1 \frac{\mu^{p+\frac{1}{2}}}{(\mu + t)^2}\, d\mu. \tag{5.13}$$

Second, using the definition of the hypergeometric function ${}_2F_1(a, b; c; x)$ [1, section 15.3] gives

$$\Theta(t) = \frac{{}_2F_1(2, p + \frac{5}{2}; p + \frac{7}{2}, -\frac{1}{t})}{(2p + 5)t} - \frac{{}_2F_1(2, p + \frac{3}{2}; p + \frac{5}{2}, -\frac{1}{t})}{2p + 3} \tag{5.14}$$

(for $p > -\frac{3}{2}$). It should be noted that when $2p$ is an integer, $\Theta(t)$ can be expressed in terms of elementary functions; for example,

$$p = -1 : \Theta(t) = -\frac{t}{1 + t}, \tag{5.15}$$

$$p = -\frac{1}{2} : \Theta(t) = -\frac{t}{2}\left(\frac{2}{1 + t} + \ln \frac{t}{1 + t}\right), \tag{5.16}$$

$$p = 0 : \Theta(t) = t + \frac{t^2}{1 + t} - 2t^{\frac{3}{2}} \arctan \frac{1}{\sqrt{t}}, \tag{5.17}$$

$$p = \frac{1}{2} : \Theta(t) = \frac{t}{2(1 + t)}\left(1 + 3t + 3t(1 + t) \ln \frac{t}{1 + t}\right), \tag{5.18}$$

$$p = 1 : \Theta(t) = \frac{t}{3} - 3t^2 - \frac{t^3}{1 + t} + 4t^{\frac{5}{2}} \arctan \frac{1}{\sqrt{t}}, \tag{5.19}$$

$$p = 2 : \Theta(t) = \frac{t}{5} - t^2 + 5t^3 + \frac{t^4}{1 + t} - 6t^{\frac{7}{2}} \arctan \frac{1}{\sqrt{t}}. \tag{5.20}$$

Figure 3 shows plots of the above $\Theta(t)$ curves at the given values of p. All plots (except for $p = -1$) show the desired characteristic of having only one strictly positive zero. Again, including a sufficiently small nonzero value of $\|b_\perp\|_2$ in the original $B(t)$ will result in a downward shift of the $\Theta(t)$ curves and will yield two positive zeros, only the smaller one of which occurs with positive $\Theta'(t)$. Thus, again we can choose a unique value for the regularization parameter. As mentioned above, $p = -1$ corresponds to a right-hand side consisting entirely of white noise, in which case the solution technique breaks down (the signal-to-noise ratio is too low).

6. Numerical examples. In order to demonstrate the ability of the zero-crossing method and how it compares to other techniques for choosing a regularization parameter, two examples from Regularization Tools [9] were considered. The first was the `shaw` example, a one-dimensional image restoration model, and the second was `deriv2`, a computation of the second derivative.

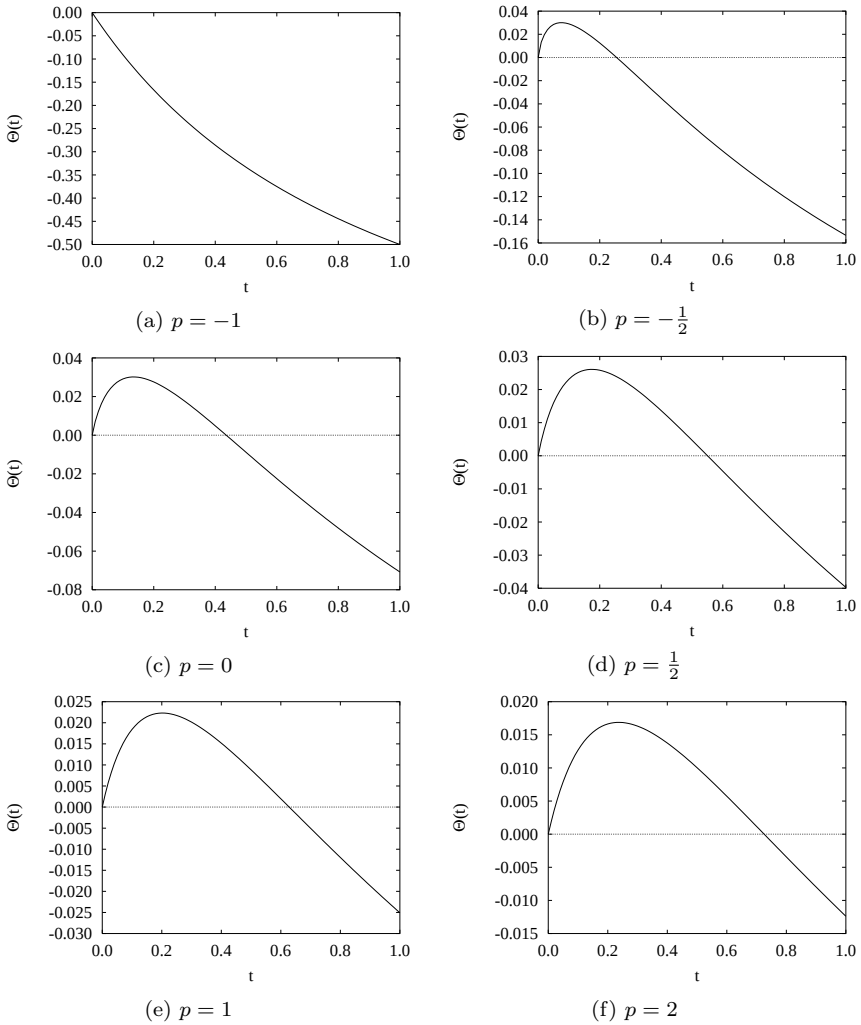

FIG. 3. *Graphs of the function $\Theta(t)$ for various values of p.*

6.1. `shaw` example. Here a 32×32 coefficient matrix was created, along with corresponding input and output vectors. Random noise of magnitude 3.2% was added to the right-hand side vector. A singular value decomposition of the coefficient matrix revealed that it had a rank of 20, indicating that $\|b_\perp\|_2 \neq 0$, and so one should look for the first zero crossing of the curve $B(t)$. Figure 4 shows plots of the function $B(t)$, the CRESO function, $C(t)$, the L-curve and the curvature of the L-curve. These curves give rise to regularization parameters which are summarized in Table 1 and compared with the optimal value. From the table it can be seen that the zero-crossing method actually predicts the optimal regularization parameter more accurately than any of the other methods. In fact, the first maximum of the CRESO function, $C(t)$, picks a completely erroneous t value.

6.2. `deriv2` example. Again a 32×32 coefficient matrix was created, along with corresponding input and output vectors, and a similar amount of noise was added to

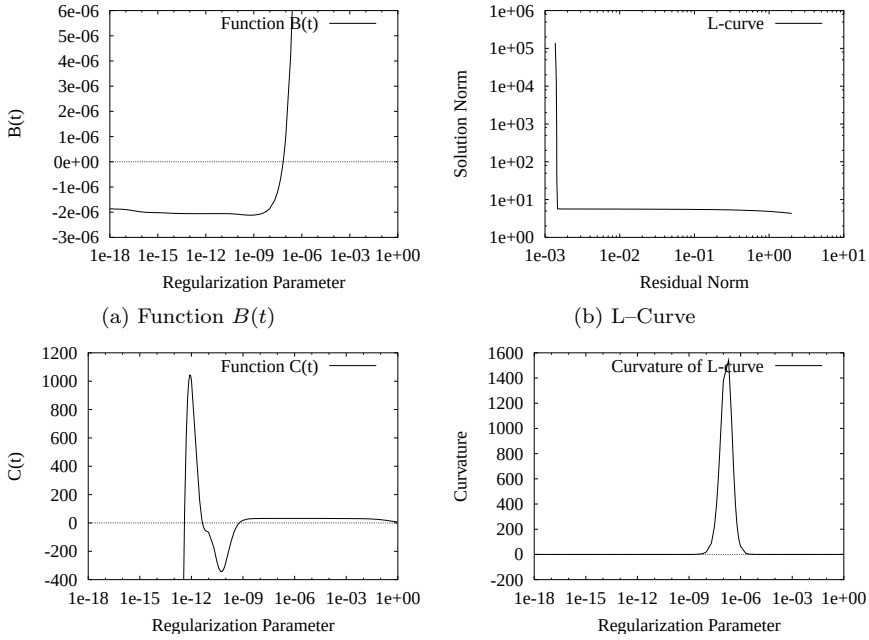

(a) Function $B(t)$ (b) L–Curve

(c) CRESO Function, $C(t)$ (d) Curvature of the L–Curve

FIG. 4. *Various curves used to determine the regularization parameter for the* `shaw` *example from Regularization Tools.*

TABLE 1
Summary of the regularization parameters obtained from different methods for the `shaw` *example.*

Curve	Regularization parameter	Relative error	Correlation coefficient
$B(t)$	7×10^{-8}	0.0526	0.9986
$C(t)$	8×10^{-13}	11.4970	0.0985
L–Curve	2×10^{-7}	0.0550	0.9985
Optimal	6×10^{-8}	0.0524	0.9986

the output. Here, a singular value decomposition revealed that the coefficient matrix was of full rank, and one would expect that $b_\perp = 0$. Hence, the appropriate zero of $B(t)$ to choose is the one with $B'(t) > 0$. Figure 5 shows the plots of the same curves as above, and Table 2 shows the different regularization parameters determined. In this example, it turns out that all three methods predict the same value of the regularization parameter, which is quite close to the optimal value.

7. Conclusion. In this paper, a formal mathematical proof has been established of the equivalence between the minimum of $\Psi_1(t)$ and the zero of the function $B(t)$ employed in the zero-crossing method. Both minimum-product and zero-crossing methods yield identical t values.

It has also been demonstrated that, under certain conditions on the Fourier coefficients of the data, the zero-crossing function $B(t)$ yields a unique regularization parameter, and hence that there is a unique minimum in the function $\Psi_1(t)$ that also corresponds to this value of t. When read in conjunction with the work of Regińska [21], it follows that under these conditions an L-curve corner also exists but may not necessarily yield the same regularization parameter on the basis of the maximum

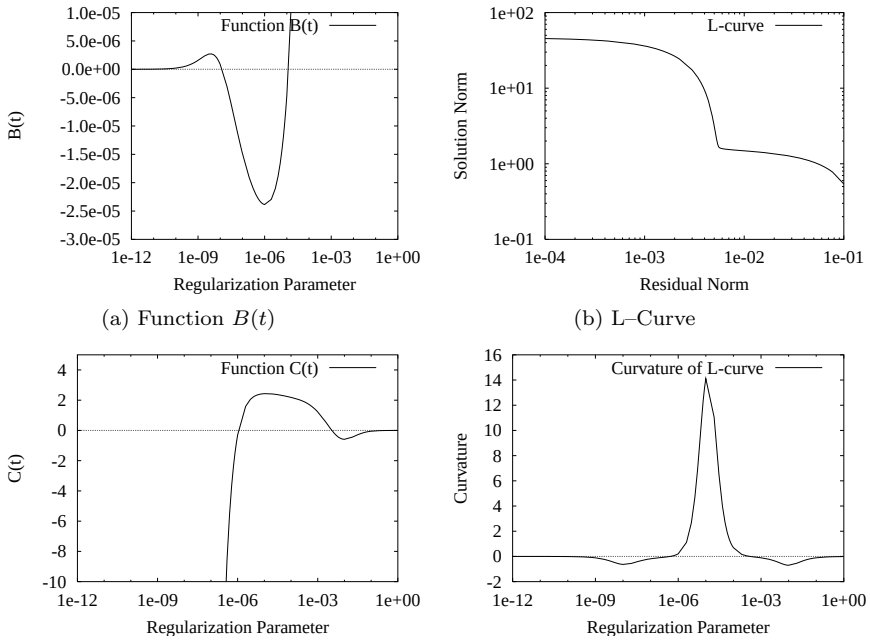

(a) Function $B(t)$ (b) L–Curve

(c) CRESO Function, $C(t)$ (d) Curvature of the L–Curve

FIG. 5. *Various curves used to determine the regularization parameter for the* `deriv2` *example from Regularization Tools.*

TABLE 2

Summary of the regularization parameters obtained from different methods for the `deriv2` *example.*

Curve	Regularization parameter	Relative error	Correlation coefficient
$B(t)$	1×10^{-5}	0.3612	0.9326
$C(t)$	1×10^{-5}	0.3612	0.9326
L–Curve	1×10^{-5}	0.3612	0.9326
Optimal	2×10^{-5}	0.3592	0.9337

curvature criterion. However, our numerical experimentation (above and in [14, 15]) has shown that the t value corresponding to the zero-crossing and minimum-product methods is close to that corresponding to the maximum curvature criterion.

Considerable numerical evidence has already been published by us [14, 15, 16] to demonstrate that the smaller strictly positive zero of $B(t)$ serves as an appropriate choice for the regularization parameter. Only under conditions where the smaller zero occurs below machine precision, conditions that correspond to geometrical errors in the coefficient matrix $\mathbf{A}$ overwhelming random measurement error in ϕ_B, does the zero-crossing method fail. Under these same conditions, our numerical simulations also indicate that there is no minimum in $\Psi_1(t)$ and no sharp corner in the L-curve, so that, in effect, all three methods for selecting t fail in unison. Until now, the zero-crossing method had remained an empirical method that worked. The theory developed here serves to put it on a more sound mathematical footing.

REFERENCES

[1] M. Abramowitz and I. A. Stegun, *Handbook of Mathematical Functions*, Dover, New York, 1965.

[2] P. Colli-Franzone, L. Guerri, B. Taccardi, and C. Viganotti, *A numerical procedure to inversely compute epicardial potentials from body surface maps applied to a normal human subject*, in Computers in Cardiology, IEEE Computer Society Press, Los Alamitos, CA, 1981, pp. 187–190.

[3] G. H. Golub, M. Heath, and G. Wahba, *Generalized cross–validation as a method for choosing a good ridge parameter*, Technometrics, 21 (1979), pp. 215–223.

[4] G. H. Golub and C. F. van Loan, *Matrix Computations*, 1st ed., The Johns Hopkins University Press, Baltimore, MD, 1983.

[5] C. W. Groetsch, *The Theory of Tikhonov Regularization for Fredholm Equations of the First Kind*, Pitman, London, 1948.

[6] C. W. Groetsch, *Inverse Problems in the Mathematical Sciences*, Vieweg, Wiesbaden, 1993.

[7] R. M. Gulrajani, F. A. Roberge, and P. Savard, *The inverse problem of electrocardiology*, in Comprehensive Electrocardiology, Vol. 1, 1st ed., Pergamon Press, 1989, pp. 237–288.

[8] P. C. Hansen, *Analysis of discrete ill-posed problems by means of the L-curve*, SIAM Rev., 34 (1992), pp. 561–580.

[9] P. C. Hansen, *Regularization Tools: A MATLAB package for analysis and solution of discrete ill-posed problems*, Numer. Algorithms, 6 (1994), pp. 1–35.

[10] P. C. Hansen, *Rank-Deficient and Discrete Ill-Posed Problems: Numerical Aspects of Linear Inversion*, SIAM, Philadelphia, 1997.

[11] P. C. Hansen, *The L-curve and its use in the numerical treatment of inverse problems*, in Computational Inverse Problems in Electrocardiography, Advances in Computational Biomedicine 5, P. R. Johnston, ed., WIT Press, Southampton, UK, 2001, pp. 119–142.

[12] P. C. Hansen and D. P. O'Leary, *The use of the L-curve in the regularization of discrete ill-posed problems*, SIAM J. Sci. Comput., 14 (1993), pp. 1487–1503.

[13] V. Isakov, *Inverse Problems for Partial Differential Equations*, Appl. Math. Sci. 127, Springer-Verlag, New York, 1998.

[14] P. R. Johnston and R. M. Gulrajani, *A new method for regularisation parameter determination in the inverse problem of electrocardiography*, IEEE Trans. Biomed. Engrg., 44 (1997), pp. 19–39.

[15] P. R. Johnston and R. M. Gulrajani, *Selecting the corner in the L–curve approach to Tikhonov regularisation*, IEEE Trans. Biomed. Engrg., 47 (2000), pp. 1293–1297.

[16] P. R. Johnston and R. M. Gulrajani, *A comparison of methods for regularisation parameter determination in the inverse problem of electrocardiography*, in Computational Inverse Problems in Electrocardiography, Advances in Computational Bioengineering 5, P. R. Johnston, ed., WIT Press, Southampton, UK, 2001, pp. 191–227.

[17] C. L. Lawson and R. J. Hanson, *Solving Least Squares Problems*, Prentice-Hall, Englewood Cliffs, NJ, 1974.

[18] J. Lian, D. Yao, and B. He, *A new method for implementation of regularisation in cortical potential imaging*, in Proceedings of the 20th Annual International Conference IEEE/EMBS, Hong Kong, 1998, pp. 2155–2158.

[19] W. Menke, *Geophysical Data Analysis: Discrete Inverse Theory*, revised ed., Academic Press, San Diego, 1989.

[20] V. A. Morozov, *Methods for Solving Incorrectly Posed Problems*, Springer-Verlag, New York, 1984.

[21] T. Regińska, *A regularization parameter in discrete ill-posed problems*, SIAM J. Sci. Comput., 17 (1996), pp. 740–749.

[22] A. N. Tikhonov and V. Y. Arsenin, *Solutions of Ill-Posed Problems*, V. H. Winston and Sons, Washington, DC, 1977.

[23] G. Wahba, *Practical approximate solutions to linear operator equations when the data are noisy*, SIAM J. Numer. Anal., 14 (1977), pp. 651–667.